frontiers | Frontiers in Chemistry

TYPE Original Research
PUBLISHED 08 December 2022
DOI 10.3389/fchem.2022.969698

OPEN ACCESS

EDITED BY
Miriam Navlani-García,
University of Alicante, Spain

REVIEWED BY
Verónica Torregrosa-Rivero,
University of Alicante, Spain
Priyanka Verma,
Shizuoka University, Japan

*CORRESPONDENCE
Aiyeshah Alhodaib,
ahdieb@qu.edu.sa
Amir Waseem,
amir@qau.edu.pk

SPECIALTY SECTION
This article was submitted to Photocatalysis and Photochemistry, a section of the journal Frontiers in Chemistry

RECEIVED 15 June 2022
ACCEPTED 28 November 2022
PUBLISHED 08 December 2022

CITATION
Ameen S, Murtaza M, Arshad M, Alhodaib A and Waseem A (2022), Perovskite $LaNiO_3/Ag_3PO_4$ heterojunction photocatalyst for the degradation of dyes.
Front. Chem. 10:969698.
doi: 10.3389/fchem.2022.969698

Perovskite $LaNiO_3/Ag_3PO_4$ heterojunction photocatalyst for the degradation of dyes

Shahzad Ameen[1], Maida Murtaza[1], Muhammad Arshad[2], Aiyeshah Alhodaib[3]* and Amir Waseem[1]*

[1]Department of Chemistry, Quaid-i-Azam University, Islamabad, Pakistan, [2]Nanosciences and Technology Department, National Centre for Physics (NCP), Quaid-i-Azam University (QAU) Campus, Islamabad, Pakistan, [3]Department of Physics, College of Science, Qassim University, Buraydah, Saudi Arabia

Pristine lanthanum nickelate ($LaNiO_3$), silver phosphate (Ag_3PO_4) and perovskite lanthanum nickelate silver phosphate composites ($LaNiO_3/Ag_3PO_4$) were prepared using the facile hydrothermal method. Three composites were synthesized by varying the percentage of $LaNiO_3$ in Ag_3PO_4. The physical properties of as-prepared samples were studied by powder X-ray diffraction (pXRD), Fourier-transform infrared (FT-IR), Scanning electron microscopy (SEM) and Energy-dispersive X-ray (EDX). Among all synthesized photocatalysts, 5% $LaNiO_3/Ag_3PO_4$ composite has been proved to be an excellent visible light photocatalyst for the degradation of dyes i.e., rhodamine B (RhB) and methyl orange (MO). The photocatalytic activity and stability of Ag_3PO_4 were also enhanced by introducing $LaNiO_3$ in Ag_3PO_4 heterojunction formation. Complete photodegradation of 50 mg/L of RhB and MO solutions using 25 mg of 5%$LaNiO_3/Ag_3PO_4$ photocatalyst was observed in just 20 min. Photodegradation of RhB and MO using 5%$LaNiO_3/Ag_3PO_4$ catalyst follows first-order kinetics with rate constants of 0.213 and 0.1804 min^{-1}, respectively. Perovskite $LaNiO_3/Ag_3PO_4$ photocatalyst showed the highest stability up to five cycles. The photodegradation mechanism suggests that the holes (h^+) and superoxide anion radicals ($O_2^{\bullet-}$) plays a main role in the dye degradation of RhB and MO.

KEYWORDS

water pollution, photocatalysis, silver phosphate, lanthanum nickelate, dyes

Introduction

The increase in the usage of inorganic and organic substances and the surge in industrialization and overpopulation have adverse effects on the soil and the quality of freshwater resources in recent years. In our daily lives, dyes are frequently used, as well as their contact with the environment is detrimental because of their risk inherent to plants, humans and wildlife (Chowdhary et al., 2020).

Water is a vital resource for human growth and life on Earth. Textile manufacturing is one of the anthropogenic processes that pollute water sources. Synthetic dyes are utilized in considerable amounts in various industries. Pharmaceutical, paint manufacturing,

cosmetics, leather and clothing industries discharge tons of various kinds of dyes into the environment (Waseem et al., 2014). During the coloring of fabric, roughly 10–15% of azo dyes do not bind and are discharged into water bodies. That's why azo dyes show more health concerns than non-azo dyes. Azo dyes are toxic for microbial communities as well as plant growth and germination. Most of these dyes are potentially non-biodegradable and extremely stable, resulting in serious environmental impacts on marine life and humans (Markandeya et al., 2017; Lellis et al., 2019).

Non-biodegradable MO is one of the common azo dyes is carcinogenic and harmful compound, if ingested, it might cause irritation of the respiratory tract, eyes and skin (Aziztyana et al., 2019; Lellis et al., 2019). In an alkaline medium, MO appears yellow, but in an acidic one, it appears red. Rhodamine B dye is commonly used in industries and is a non-biodegradable dye, causes numerous environmental contamination issues by releasing carcinogenic and harmful compounds into the water. If RhB is ingested, it might cause irritation of the abdominal disorders, blindness, respiratory distress and skin sensitization. (Markandeya et al., 2017; Areeb et al., 2021). In an alkaline medium, RhB appears colorless, but in an acidic one, it appears pink. Methyl orange is a type of azo dye that is commonly used in textiles.

Due to their high-water solubility, dyes and organic chemicals such as dyes are difficult to remove using traditional methods. To decompose dyes and other organic substances in water, different treatment techniques have been used. Toxins are extracted from wastewater in different ways by each approach. Major methods include 1) Chemical methods such as chlorination and ozonation, 2) Physical methods such as ultra-filtration, adsorption, reverse osmosis and ion exchange, 3) Biological methods such as aerobic as well as anaerobic treatments (Maheshwari et al., 2021). The majority of the traditional approaches just change the phase of chemicals without transforming them into eco-friendly products. As a result, their application is not compatible since they produce harmful side products that require additional treatment, bringing excessive expense to the degradation process (Katheresan et al., 2018).

Photoreactions of semiconductors due to their greater potential to mineralize organic pollutants in the environment have become highly significant among the various Advanced Oxidation Processes (AOPs) in recent years (Szczepanik, 2017). Among the numerous novel technologies accessible today, the use of materials for heterogeneous photocatalysis/electrocatalysis has been regarded as one of the most efficient methods for tackling both energy as well as environmental challenges and has thus gained a lot of attention in recent years (Gao et al., 2021; Wu et al., 2021). Due to their good magnetic, physical and optical properties, a number of nanostructured semiconductors such as ZnS, ZnO, CdS, TiO_2 and WO_3 are used as photocatalysts (Sudha and Sivakumar, 2015; Luo et al., 2019; Saravanan et al., 2020).

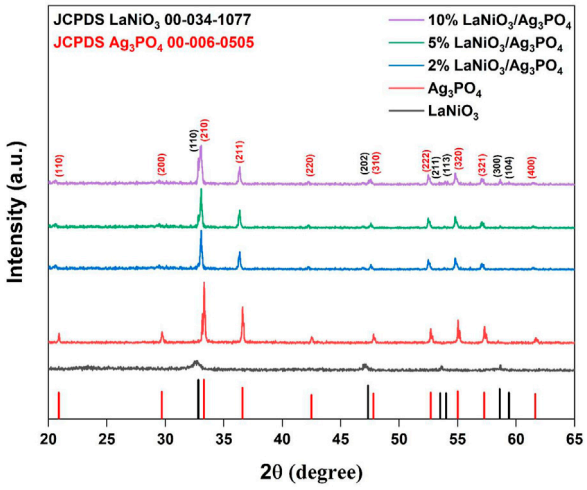

FIGURE 1
Powder XRD pattern of $LaNiO_3$, Ag_3PO_4, 2% $LaNiO_3/Ag_3PO_4$, 5% $LaNiO_3/Ag_3PO_4$ and 10% $LaNiO_3/Ag_3PO_4$ composite.

Under visible light, silver orthophosphate (Ag_3PO_4) has a very strong photocatalytic activity. According to charge neutrality analysis, Ag_3PO_4 may act as a weakly p-type semiconductor for O-rich conditions and as a weakly n-type semiconductor for O-poor conditions (Reunchan and Umezawa, 2013), and has a band gap of 2.36 eV semiconductor with good visible light degradation of organic pollutants and induced oxygen evolution (Li et al., 2019). However, due few disadvantages of silver phosphate such as: photogenerated electrons can easily reduce Ag^+ in Ag_3PO_4 to elemental silver (Ag^0), and electron-hole pair recombination. (Zhang et al., 2014; Chen et al., 2022). The composite formation is an effective method for expanding absorption from ultraviolet to visible region that either adds a new band into the initial band or alters the valence band (VB) or conduction band (CB), improving photocatalytic activity (Zhang et al., 2017; Lv et al., 2019). Composite formation of Ag_3PO_4 with other materials such as carbon nanotubes (Xu et al., 2014), graphene oxide (Chen G. et al., 2013) have also been reported in recent years. Similarly, combining other semiconductors with Ag_3PO_4 to form a heterojunction is also a promising strategy. For example, $Bi_4Ti_3O_{12}/Ag_3PO_4$ (Zheng et al., 2017), TiO_2/Ag_3PO_4 (Liu et al., 2019), $ZnWO_4/Ag_3PO_4$ (Zhang et al., 2017), $BiVO_4/Ag_3PO_4$ (Qi et al., 2016) *etc.* The advantages of coupled semiconductors include extending the light responsive range and boosting the transferring abilities of the photo-generated charge carrier.

In this study, the stability and photocatalytic activity of Ag_3PO_4 is enhanced by composite formation with $LaNiO_3$, ABO_3 type perovskite. Perovskites are another appealing semiconductor photocatalyst with changeable components, simple structure, and good stability (Grabowska, 2016; Zhang

et al., 2016). The theoretical bandgap energy (2.40 eV) of $LaNiO_3$ allows it to absorb visible light energy, but in actual practice, the photocatalytic activity of pure $LaNiO_3$ is not as good as expected due to poor response to visible light and electron and hole pair recombination (Gao et al., 2019). Combining $LaNiO_3$ with Ag_3PO_4 shows a facile way to improve photocatalytic activity and stability for water treatment.

Experimental

Materials

Sodium hydroxide (NaOH), Lanthanum nitrate hexahydrate ($La(NO_3)_3 \cdot 6H_2O$) and Nickel nitrate hexahydrate ($Ni(NO_3)_2 \cdot 6H_2O$) were purchased from Sigma Aldrich. ethanol (CH_3CH_2OH) was obtained from Merk (Germany). Silver nitrate ($AgNO_3$) and Sodium phosphate (Na_3PO_4) were provided by Sigma-Aldrich. All the chemicals were of analytical grade, and all the solutions were prepared in distilled water.

Synthesis of perovskite $LaNiO_3$

Perovskite $LaNiO_3$ was prepared by the facile hydrothermal method. In a typical synthesis, stoichiometry amounts of lanthanum nitrate hexahydrate and nickel nitrate hexahydrate were mixed in distilled water under stirring conditions. Sodium hydroxide was added to maintain the pH 11. The resulting mixture was transferred into an autoclave for hydrothermal treatment at 180°C for 12 h. The product was washed with distilled water and ethanol and dried overnight. Then the product was calcined at 650°C for 4 hours in order to obtain the lanthanum nickelate powder.

Synthesis of perovskite $LaNiO_3/Ag_3PO_4$ composites

Composites of lanthanum nickelate and silver phosphate were prepared by the hydrothermal method (Guan and Guo, 2014). In a typical procedure, an appropriate amount of lanthanum nickelate was dispersed in distilled water by sonication, stoichiometry amounts of silver nitrate and sodium phosphate were added in the mixture. The yellow precipitates of silver phosphate were observed. Immediately the mixture was transferred into Teflon lined autoclave for 24 h at 100°C. The obtained composite was washed with water and ethanol. Three composites were obtained by varying the amounts of lanthanum nickelate and labeled as 2% $LaNiO_3/Ag_3PO_4$, 5% $LaNiO_3/Ag_3PO_4$ and 10% $LaNiO_3/Ag_3PO_4$. Pure silver phosphate was prepared by same procedure without adding lanthanum nickelate.

Procedure for the measurement of catalytic performance

The efficiency of as prepared photocatalysts was examined by the photodegradation of RhB and MO under visible light (using 100 watts LED light with an output of 40 k Lux, measured with Extech LT300 light meter). In a typical procedure, 0.025 g of $LaNiO_3/Ag_3PO_4$ photocatalyst is added to the solution of RhB and MO (25 ppm) under stirring conditions using a magnetic stirrer at room temperature. Suspensions were collected at given time intervals, and the photocatalyst was removed with the help of a centrifuge (4,000 rpm, 5 min). UV–Vis spectrophotometer (Model UV-1700 SHIMADZU) was used to determine the concentration of residual RhB and MO in supernatant solution depending on the highest absorption of RhB and MO at wavelengths of 554 and 464 nm, respectively. Degradation efficiency was calculated using the following relationship.

$$\mathbf{DegradationEfficiency}\,(\%) = \frac{(\mathbf{C_o} - \mathbf{Ct})}{\mathbf{C_o}} \times \mathbf{100}, \qquad (1)$$

Where C_t is concentration after time t and C_o is the initial concentration.

Results and discussion

Powder X-ray diffraction analysis

The diffraction pattern of $LaNiO_3$ shows 2theta values of 32.8°, 47.3°, 53.5°, 54.1°, and are well matched with the rhombohedral phase of $LaNiO_3$ (JCPDS No.00-034-1077; space group, R), while those of Ag_3PO_4 corresponded to 2theta values of 20.9°, 29.7°, 33.2°, 36.5°, 47.7°, 52.7°, 57.1° shows the cubic structure of Ag_3PO_4 (JCPDS No.00-006-0505; space group, $P\bar{4}3n$). The XRD pattern of $LaNiO_3/Ag_3PO_4$ composites showed a combination of $LaNiO_3$ and Ag_3PO_4 and ruled out the possibility of other impurity phases, indicating successful synthesis of composite. Furthermore, it is observed that the diffraction peaks of $LaNiO_3$ gradually strengthened with increasing the $LaNiO_3$ content, while the peak intensities of Ag_3PO_4 weakened. The hydrothermal treatment gave well-crystallized Ag_3PO_4 particles with sharp diffraction peaks. Compared to Ag_3PO_4, peaks of $LaNiO_3$ were broader and less sharp, which may be resulting from smaller crystallite size (Figure 1). The crystallite size of 14.7 nm, 86.5 nm, 58.1 nm were calculated for $LaNiO_3$, Ag_3PO_4 and 5% $LaNiO_3/Ag_3PO_4$ composite respectively using Scherrer equation.

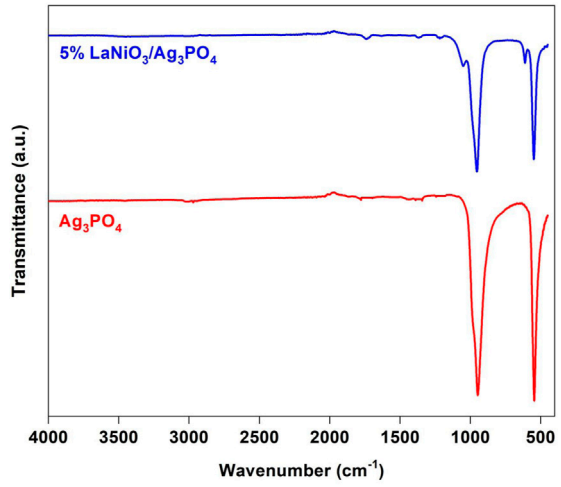

FIGURE 2
FT-IR spectra of Ag_3PO_4 and 5% $LaNiO_3/Ag_3PO_4$.

FT-IR spectroscopy

Figure 2 shows the FT-IR spectra of Ag_3PO_4 and 5% $LaNiO_3/Ag_3PO_4$. In the spectrum of silver phosphate, two strong peaks were observed at 550 cm^{-1} and 946 cm^{-1} and were assignable to bending and stretching vibrations of the P-O bond, respectively. Two small peaks at 565 cm^{-1} and 965 cm^{-1} is observed for bending vibrations of Ni-O bond.

Scanning electron microscopy

SEM was used to investigate the morphology and particle size of as-prepared samples. SEM images of 5% $LaNiO_3/Ag_3PO_4$ showed that particles of $LaNiO_3$ were uniformly and tightly attached on the surface of Ag_3PO_4, which indicated an intimate contact between $LaNiO_3$ and Ag_3PO_4. Pure Ag_3PO_4 possessed a polyhedral morphology and has interstitial spaces, as shown in Figures 3A,B, whereas, these spaces were filled with $LaNiO_3$ accumulation in 5% $LaNiO_3/Ag_3PO_4$ composite. Figures 3E,F shows the very tiny particles of $LaNiO_3$. Figures 3C,D showed that $LaNiO_3$ particles are uniformly distributed on the surface of Ag_3PO_4.

Energy-dispersive X-ray spectroscopy

EDX was used to find the elemental composition of Ag_3PO_4 and $LaNiO_3/Ag_3PO_4$ composite. Figure 4 depicted the elemental composition of Ag_3PO_4 and 5%$LaNiO_3/Ag_3PO_4$ composite. The EDX Ag_3PO_4 shows (wt%) Ag = 77, p = 7.3, O = 15.7, whereas 5% $LaNiO_3/Ag_3PO_4$ shows (wt%) Ag = 73.1, p = 6.9, La = 2.9, Ni = 1.2, O = 15.8. The energy-dispersive X-ray spectrum of composite shows that La, Ni, Ag, P, and O are present in the composite and confirmed the successful synthesis of the composite.

Band gap estimation and optical study

When light falls on the surface of semiconductor photocatalyst electrons move from VB to CB by absorbing energy. The relationship between the band gap energy and absorption spectra can be represented by Tauc equation which is written as:

$$(\alpha h\upsilon) = k\left(h\upsilon - E_g\right)^n$$

where $h\upsilon$ is the energy of photon, n is a type of transition, and n is either 1/2 for a direct transition or 2 for an indirect transition, k is the band tailing parameter, that does not dependent on energy, and E_g is the energy of band gap (Masnadi-Shirazi et al., 2014). The Beer-Lambert law can be used to calculate coefficient of absorption (α). Band gap value (E_g) between the wavelength ranges from 200 to 800 nm can be quantified by extrapolating linear region of plot energy (hυ) vs $(\alpha h\upsilon)^2$. Different parameters such as doping, grain size, annealing treatment and type of transition (direct or indirect), create differences in Eg values (Hameeda et al., 2021). The band gap energies of Ag_3PO_4 and $LaNiO_3$ were found to be 2.36 and 2.40 eV respectively, which are similar to previous findings (Li et al., 2019; Chen et al., 2022). These photocatalysts have comparable band gap energies. The band gap energy of 5% $LaNiO_3/Ag_3PO_4$ composite is 2.38 eV. Tauc plots of Ag_3PO_4, $LaNiO_3$ and 5% $LaNiO_3/Ag_3PO_4$ are depicted in the Figures 5A–C respectively.

Optimization studies for rhodamine B photodegradation

The purpose of this work is to investigate new avenues in the study of photodegradation efficiency of highly effective and freshly synthesized photocatalysts for rhodamine B (RhB) degradation using various parameters such as pH, catalyst dose, time and concentration of dye. The effect of dye adsorption in dark was also studied and it was observed that no significant adsorption was observed in the absence of light.

The photocatalytic activity of as-prepared catalysts for rhodamine B degradation was investigated with UV-Visible spectrophotometry, by taking 25 mg of the each photocatalyst and 30 ml of RhB solution (25 mg/L). The resultant solutions were exposed to light lasting 20 min while being continuously magnetically stirred. The most appropriate catalyst was selected based on their performance for dye degradation. The absorption spectrum of RhB from photocatalytic studies was observed between the wavelength ranges from 200 to 600 nm. After a

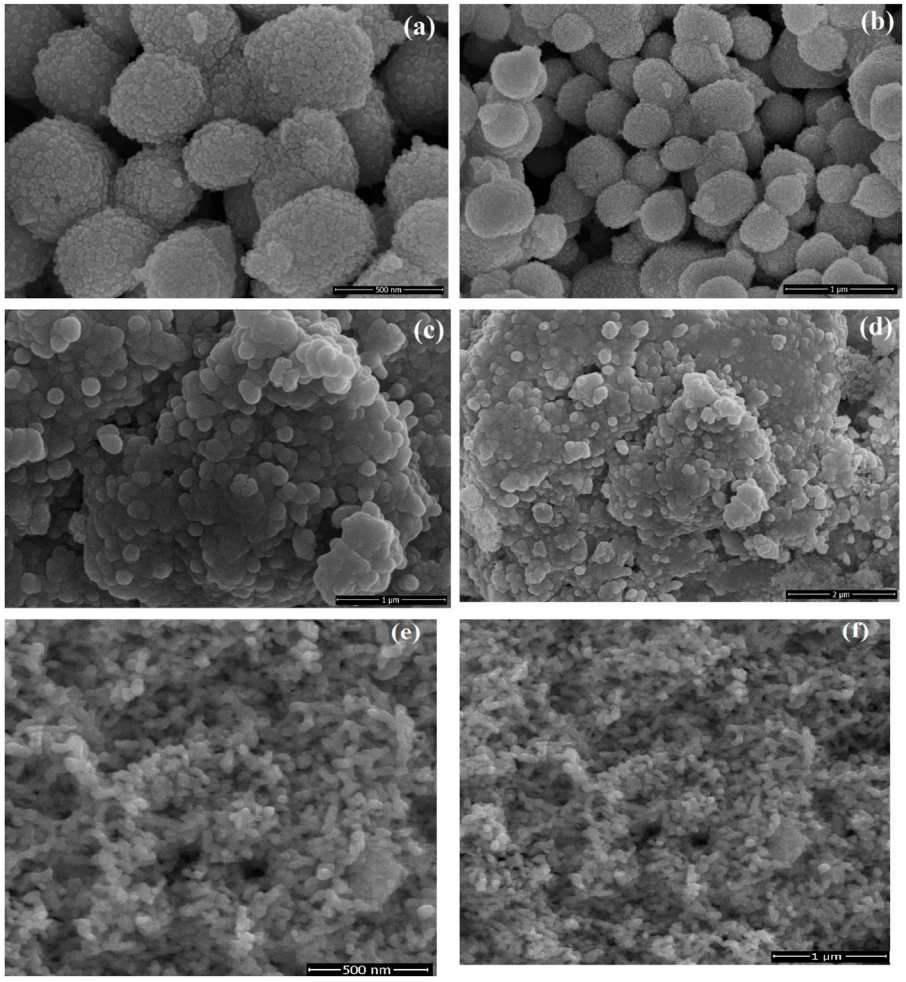

FIGURE 3
SEM images of Ag_3PO_4 **(A,B)**, and $LaNiO_3/Ag_3PO_4$ composite **(C,D)**, $LaNiO_3$ **(E,F)** at different resolutions.

specified period of time, the strength of the RhB distinctive peak began to decrease (Figure 6A). The optimum catalyst was selected depending on the efficiency of dye degradation. The photocatalytic activity increases by increasing the content of $LaNiO_3$ in the $LaNiO_3/Ag_3PO_4$ composite up to 5% but it decreases by further increasing the $LaNiO_3$ content due to the possible formation of agglomeration. The results demonstrate that the $2\%LaNiO_3/Ag_3PO_4$ and $10\%LaNiO_3/Ag_3PO_4$ composite showed higher activity than pure $LaNiO_3$ and Ag_3PO_4 but lower than 5% $LaNiO_3/Ag_3PO_4$ composite. Therefore, $5\%LaNiO_3/Ag_3PO_4$ composite was found to be good photocatalyst for the degradation of rhodamine B providing good stability and synergy for photocatalysis.

pH of the solution is an important parameter in studying the degradation reaction. The surface charges of the photocatalyst are directly affected by pH. The RhB solution's pH was regulated using 1 M sodium hydroxide and 1 M hydrochloric acid solution. The pH of the solution is adjusted at the commencement of the reaction. The photodegradation investigation was conducted under the conditions: (Irradiation time: 20 min, amount of catalyst: 25 mg, solution's pH: 2–10, concentration of RhB: 25 mg/L). According to Figure 6B the degradation efficiency of RhB using $5\%LaNiO_3/Ag_3PO_4$ photocatalyst is maximum at pH 7. The pH of solution is a major factor in photocatalytic process that occurs on the surface of a photocatalyst because it determines the surface charge properties of the photocatalyst as well as the size of aggregate particles that form. As a result, pH plays a significant influence in the reaction pathways that can lead to the degradation of dye. Photocatalytic activities are likely to emerge in the existence of catalyst through electron-hole pairs generated on the photocatalysts surface by visible light irradiation. The effect of pH on the dye degradation varies greatly depending on the photocatalyst available in the water. According to prior research, the surface of Ag_3PO_4 catalyst is

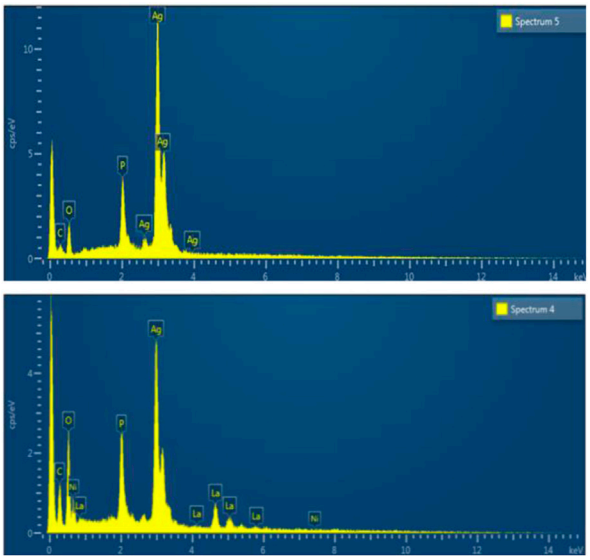

FIGURE 4
EDX spectrum of (upper) Ag_3PO_4 (lower) 5%$LaNiO_3$.

neutral at pH 5.4. In acidic conditions, the surface of photocatalyst is positively charged, whereas in alkaline media, it is negatively charged. The highest degradation efficiency of RhB was achieved in neutral solutions (pH 7), but it was less efficient in alkaline medium. Despite being a cationic dye, rhodamine B has a low degradation in basic solutions (above pH 7), and the surface of catalyst is negatively charged at the pH above 5.4. This strange behavior can be attributed to the fact that silver ions in silver phosphate reduced to elemental silver which reduces the active site of the catalyst and degradation efficiency decreases.

Degradation of RhB with 5%$LaNiO_3$/Ag_3PO_4 photocatalyst was examined for time optimization under visible light irradiation. Photodegradation experiment was conducted out under the conditions: (Irradiation time: 0–20 min, amount of catalyst: 25 mg, solution's pH: 7, concentration of RhB: 25 mg/L). As seen in Figure 6C a typical absorption peak of RhB rapidly diminishes as the exposure period increases, associated with rapid change in color of dye solution. Increased exposure time to the light improves rate of electron flow from valence to the conduction band, resulting in increased degradation efficiency. After 20 min, RhB was found to have entirely degraded.

It is critical to obtain information on the optimum quantity of catalyst to be used in the reaction, not only to determine its cost, but also to ensure that it is recovered after the reaction is completed. With this in mind, the effect of catalyst quantity on RhB degradation was investigated. The photodegradation experiment was conducted out under the conditions: (Irradiation time: 20 min, amount of catalyst: 10–30 mg, solution's pH: 7, concentration of RhB: 25 mg/L). Figure 6D

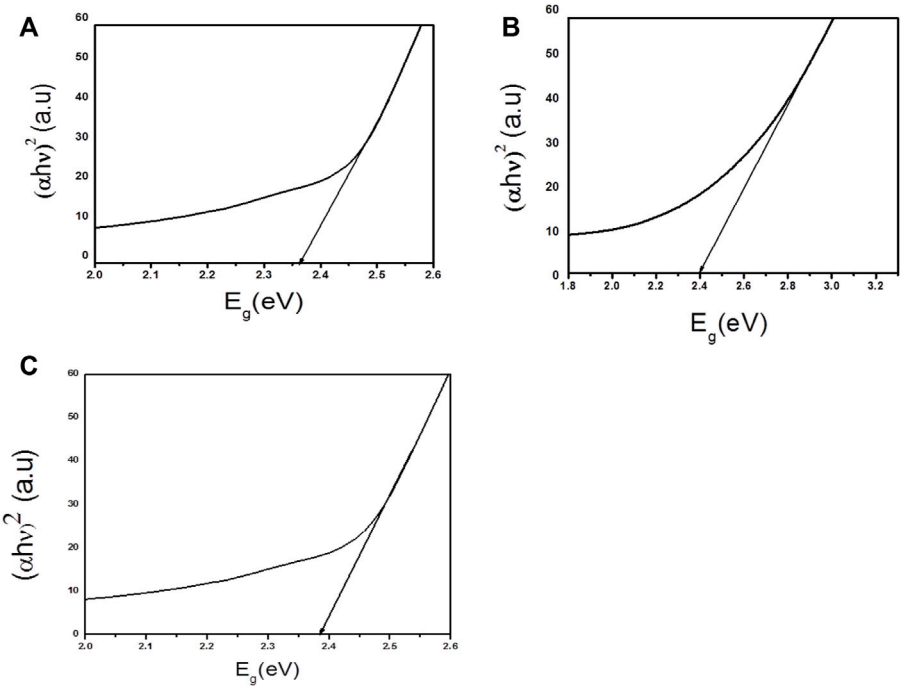

FIGURE 5
Tauc plots of **(A)** Ag_3PO_4 **(B)** $LaNiO_3$ **(C)** 5% $LaNiO_3$/Ag_3PO_4.

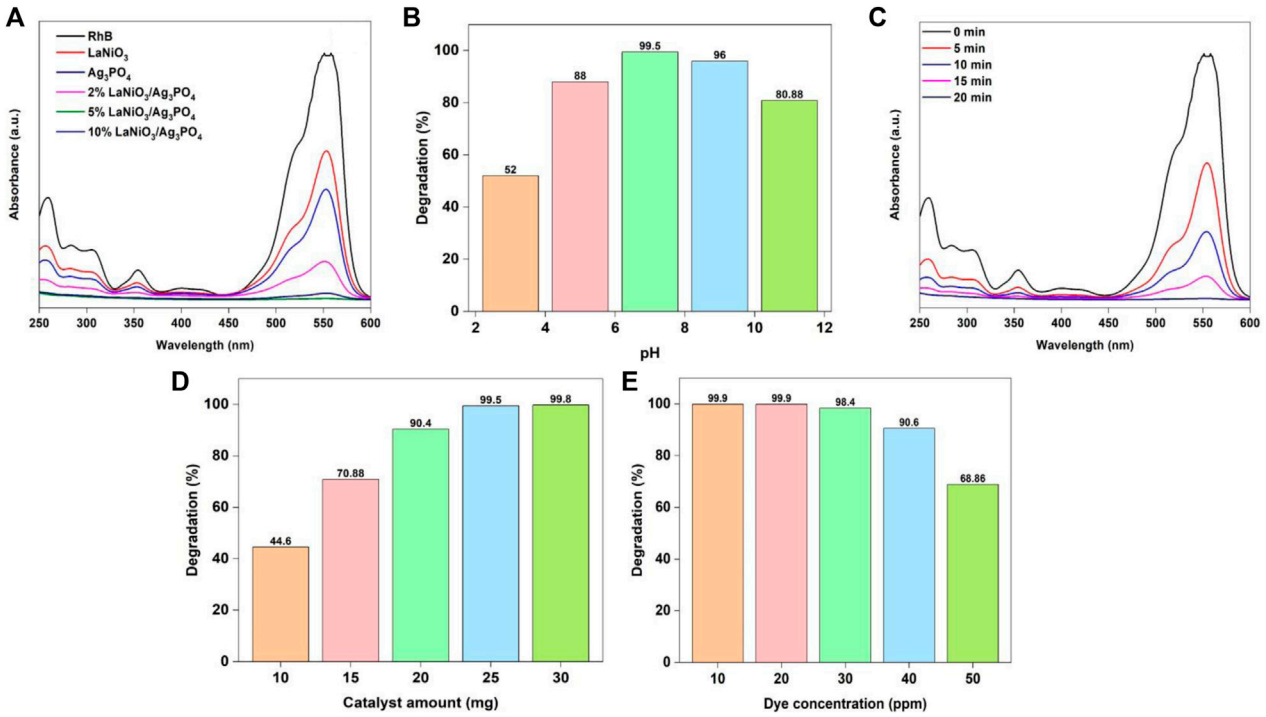

FIGURE 6
Change of RhB degradation efficiency of photocatalysts with **(A)** type of catalyst, **(B)** pH **(C)** time, **(D)** catalyst amount **(E)** dye concentration. Reaction conditions: Light Source: 100 watts LED, Intensity: 40 k Lux, temperature: 25°C, Pressure: 1 atm.

depicts the influence of catalyst quantity on RhB degradation efficiency. It was found that by adding 5%$LaNiO_3/Ag_3PO_4$ photocatalyst to reaction mixture had a significant impact on the process efficiency. The percentage of degradation rose as the catalyst dose increased, maximum at 25 mg of catalyst. The rise in the efficiency of degradation is due to the catalyst's active sites increasing, resulting in the generation of more reactive radicals (superoxide anion and hydroxyl) that drive the degradation process.

RhB photodegradation efficiency was further studied by varying the concentrations of RhB under visible light irradiation. Photodegradation experiment was conducted out under the conditions: (Irradiation time: 20 min, amount of catalyst: 25 mg, solution's pH: 7, concentration of RhB: 10–50 mg/L). The photodegradation reaction was shown to slow down as concentrations of RhB increased. This can happen when O_2 adsorption is decreased due to higher dye molecules adsorption on the surface of the catalyst, resulting in a reduction of photocatalyst active sites, and thus the production of extremely oxidative $^{\bullet}O_2^-$ is inhibited. Furthermore, high concentrations of dye cause light to self-absorb, preventing it from reaching the surface of catalyst. As a result, insufficient energy from photons reaches the catalyst's active sites, leading to lower efficiency. In addition to that, because of the high concentration of RhB, intermediate compounds may form during the photodegradation reaction and absorb certain active radicals that may interact with the molecules of dye. Therefore, the overall degradation efficiency decreases. The degradation efficiency is still good up to 90.5% using 50 mg/L of RhB (Figure 6E).

Optimization studies for methyl orange photodegradation

To investigate the photodegradation efficiency of highly effective and freshly synthesized photocatalysts for methyl orange (MO) degradation, various parameters such as catalyst type, pH, catalyst dose, time and dye concentration were carried out. The effect of dye adsorption in dark was also studied and it was observed that no significant adsorption was observed in the absence of light.

The photocatalytic activity of as-prepared samples for MO degradation was investigated with UV-Vis spectrophotometry, by using 25 mg of the each photocatalyst and 30 ml of MO solution (30 ppm). The resultant solutions were exposed to light for 25 min with continuous stirring. The most appropriate catalyst was selected based on their performance for dye

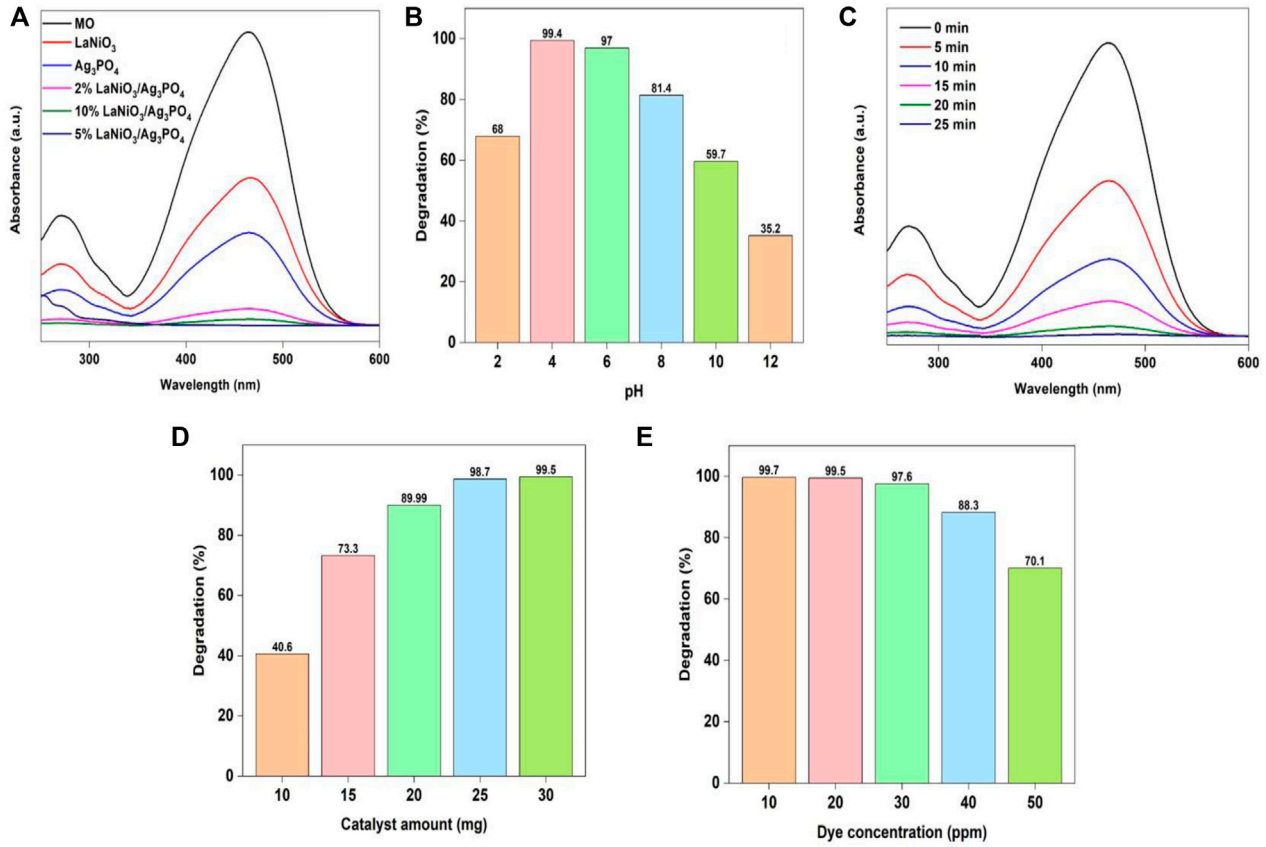

FIGURE 7
Change of MO degradation efficiency with variable **(A)** type of catalyst, **(B)** pH **(C)** time, **(D)** catalyst amount **(E)** dye concentration. Reaction conditions: Light Source: 100 watts LED, Intensity: 40 k Lux, temperature: 25°C, Pressure: 1 atm.

degradation. The absorption spectrum of MO from photocatalytic studies was observed between the wavelength ranges from 200 to 600 nm. After some time, the strength of the MO distinctive peak began to decrease. The activity was increased by increasing the content of $LaNiO_3$ in the $LaNiO_3$/Ag_3PO_4 composite up to 5% but it decreased by further increasing the $LaNiO_3$ content possibly due to agglomeration (Figure 7A). The results demonstrate that the 2% $LaNiO_3$/Ag_3PO_4 and 10% $LaNiO_3$/Ag_3PO_4 composite showed higher activity than pure $LaNiO_3$ and Ag_3PO_4 but lower than 5% $LaNiO_3$/Ag_3PO_4 composite. Therefore, 5% $LaNiO_3$/Ag_3PO_4 composite was found to be suitable photocatalyst for the degradation of MO.

Further investigations were carried out to check the influence of pH on MO photodegradation. The photodegradation experiment was conducted out under the conditions: (Irradiation time: 25 min, amount of catalyst: 25 mg, solution's pH: 2–12, concentration of MO 30 mg/L).

Figure 7B shows that the percentage efficiency for the removal of MO dye with 5%$LaNiO_3$/Ag_3PO_4 is highest at pH 4. Because pH affects multiple variables, including ionization state of the photocatalyst and dye, ease of producing hydroxyl radicals, and catalyst agglomeration, it is referred to as a complicated parameter (Akpan and Hameed, 2009). Because photocatalytic reaction takes place predominantly on the surface of photocatalyst, the surface parameters have a significant effect on the performance of catalyst. Surface of the photocatalyst is positively charged in acidic conditions, and azo structure of methyl orange is also transformed into quinoid structure in acidic conditions. The quinoid structure of Methyl Orange is easy to degrade than azo structure as reported in literature (Basahel et al., 2015). Acidic condition promoted the degradation reaction catalyzed by 5%$LaNiO_3$/Ag_3PO_4. Electrostatic interactions among the dye molecules and the surface of catalyst are also important in the degradation process. The increased efficiency in acidic conditions is explained by the anionic character of MO and absorption of H^+ ions on the surface of catalyst. Under acidic conditions, the MO is easily absorbed on the surface of photocatalyst which is positively charged. In acidic media,

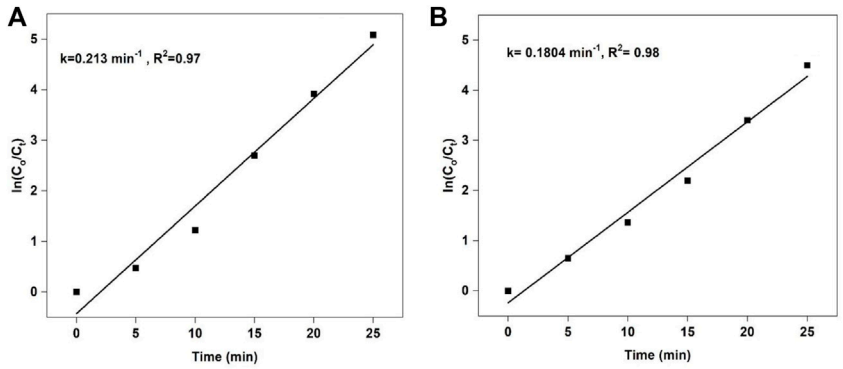

FIGURE 8
Pseudo first order kinetics of RhB **(A)** k = 0.2130 ± 0.0126, MO **(B)** k = 0.1804 ± 0.0113 Reaction conditions: Light Source: 100 watts LED, Intensity: 40 k Lux, temperature: 25°C, Pressure: 1 atm. Catalyst amount: 25 mg, Dye concentration: 30 mg, pH: Neutral.

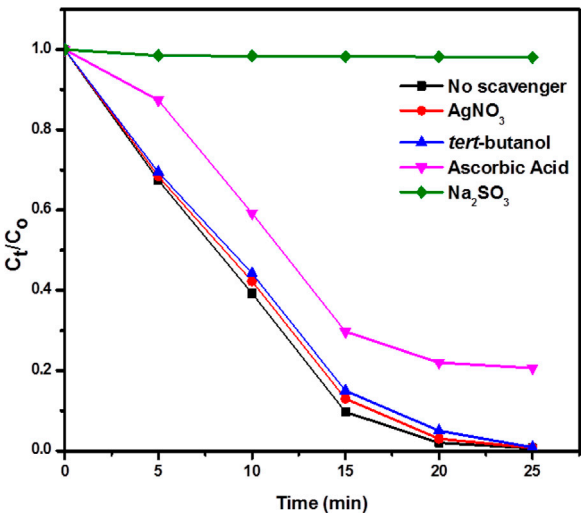

FIGURE 9
The effect of different scavengers on dye degradation of RhB. Reaction conditions: Light Source: 100 watts LED, Intensity: 40 k Lux, temperature: 25°C, Pressure: 1 atm. Catalyst amount: 25 mg, Dye concentration: 30 mg.

removal of MO is more effective than in alkaline media (Mansouri et al., 2019).

The influence of reaction time on MO photodegradation was further investigated with the following conditions: (Irradiation time: 0–20 min, amount of catalyst: 25 mg, solution's pH: 4, concentration of MO: 30 mg/L). Figure 7C shows that by extending the irradiation time, the efficiency of MO removal increases. Irradiation time of 20 min was selected for further study due to highest degradation efficiency for MO using the specified reaction conditions. To assess the amount of catalyst for the photocatalytic degradation of MO, the effect of catalyst dose was further investigated under the conditions: (Irradiation time: 20 min, amount of catalyst: 10–30 mg, solution's pH: 4, concentration of MO 30 mg/L). The results showed that increasing the catalyst amount significantly increased capability of dye adsorption as well as rate of photodegradation. As shown in Figure 7D that increasing the catalyst dosage from 10 to 30 mg significantly enhances dye degradation efficiency. It is clearly seen that raising the photocatalyst amount increases the availability of active sites as well as illuminated area available for the degradation of extra dye molecules and adsorption. As a result, as the catalyst dosage was increased, the rate of photodegradation rose.

To investigate the influence of dye concentrations on photodegradation reaction, the photodegradation experiment was conducted under following conditions: (Irradiation time: 20 min, amount of catalyst: 25 mg, solution's pH: 4, concentration of MO: 20–60 mg/L). A photodegradation process was shown to decrease as dye concentration increased, as illustrated in Figure 7E. This decrease in the rate of degradation with increasing dye concentration may be ascribed to the higher dye concentration reducing the active catalyst due to saturation effect. Furthermore, increasing the concentration of dye would enhance dye molecules adsorption on the photocatalyst surface and avoid the adsorption of oxygen and hydroxyl ions on the surface of photocatalyst for photodegradation.

Degradation kinetics

To find the order and rate constant of degradation reaction, we have studied the degradation kinetics. The degradation reaction of rhodamine B by 5%$LaNiO_3$/Ag_3PO_4 composite follows pseudo 1st order kinetic having rate constant

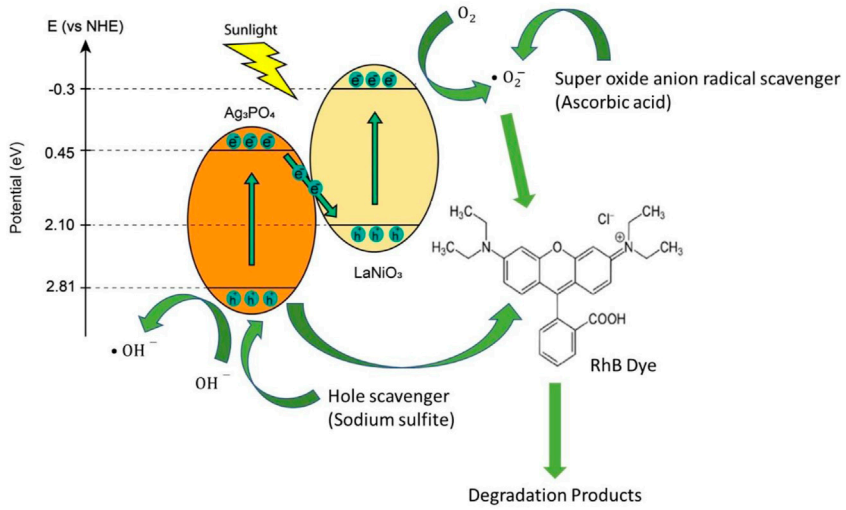

FIGURE 10
The possible mechanism for dye degradation.

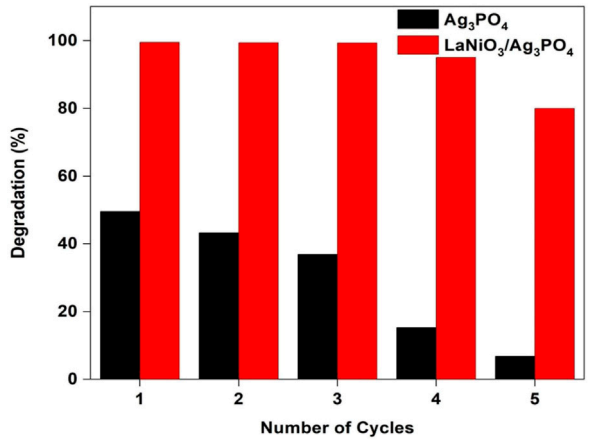

FIGURE 11
The stability of the photocatalyst with the number of cycles.

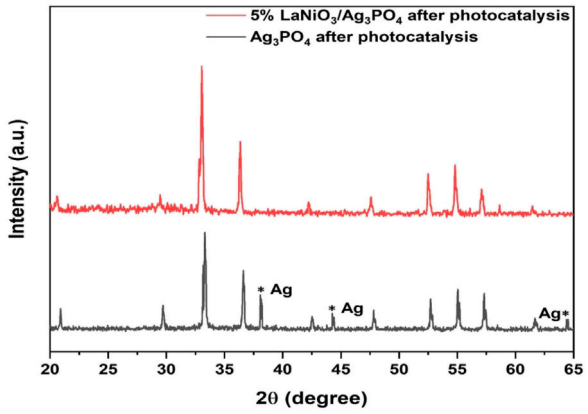

FIGURE 12
Powder XRD pattern of Ag_3PO_4, 5% $LaNiO_3/Ag_3PO_4$ composite after photocatalysis.

0.213 min^{-1}. Whereas, the methyl orange degradation reaction by 5%$LaNiO_3/Ag_3PO_4$ composite also shows pseudo 1st order kinetics with a rate constant of 0.180 min^{-1} as shown in Figures 8A,B).

Possible mechanism for the photocatalytic dyes degradation

In order to understand the mechanism for the degradation of RhB and MO, the effect of different scavengers on RhB and MO degradation was carried out. Figure 9 shows that photocatalytic activity is completely inhibited by using hole scavenger sodium sulfite, but it remains almost unchanged by using electron scavenger ($AgNO_3$). It means that holes play a crucial role in the degradation of RhB and MO. In the photodegradation system, the superoxide anion radical ($O_2^{\bullet-}$) radicals are effective reactive oxygen species, which are produced by the reduction of O_2 molecules adsorbed on the catalyst surface by the photogenerated electrons (Luo et al., 2019). Photocatalytic activity slightly changed by adding superoxide anion radical scavenger ascorbic acid while it remains unchanged by adding hydroxyl radical scavenger *tert*-butanol (TBA). So, superoxide anion radicals also play a role in the dye degradation of RhB and MO.

TABLE 1 Comparison of RhB photodegradation by various catalysts from the literature.

Catalyst	Catalyst amount (mg)	Dye amount (mg/L)	Degradation time (min)	Degradation efficiency (%)	Rate constant (min^{-1})	References
Ag_3PO_4@GO	50	6	60	99	–	Liu et al. (2018)
Ag_3PO_4/WO_3	40	5	30	97	–	Zhang et al. (2014)
Ag_3PO_4/Ag	100	10	90	98	–	Huang et al. (2015)
Ag_3PO_4/ZnO	20	10	30	93	0.0895	Dong et al. (2014)
$LaNiO_3$	10	10	120	53	0.006	Ghafoor et al. (2021)
Ag_3PO_4/ N-TiO_2	20	10	120	99	0.0194	Khalid et al. (2020)
$Ag_3PO_4/BiVO_4$	100	10	30	92	0.088	Qi et al. (2016)
Ag_2MoO_4/ Ag_3PO_4	50	10	12	97	0.3591	Cao et al. (2017)
$AgBr/Ag_3PO_4$	100	10	7	99	–	Wang et al. (2013)
$Bi_4Ti_3O_4$/ Ag_3PO_4	20	5	30	99	0.1789	Zheng et al. (2017)
g-C_3N_4/ Ag_3PO_4	100	10	10	96	–	He et al. (2014)
Ag_3PO_4/ $CdWO_4$	100	10	5	99	0.71	Zhang et al. (2020)
CNT/Ag_3PO_4	75	10	12	92.4	0.207	Xu et al. (2014)
$LaNiO_3$/ Ag_3PO_4	25	50	20	90.5	0.213	Present Study

Energy band positions of $LaNiO_3$ and Ag_3PO_4 are shown in the Figure 10. The valence band positions of $LaNiO_3$ and Ag_3PO_4 are 2.10 eV and 2.81 eV while conduction band positions are −0.3 eV and 0.45 eV respectively. Here, Z-Scheme heterostructure is formed between $LaNiO_3$ and Ag_3PO_4. When the light falls on the surface of the photocatalyst, electrons from valence band of Ag_3PO_4 move towards conduction band of $LaNiO_3$. Therefore, holes and electrons are formed (Ge et al., 2012; Khalid et al., 2020).

$$hv + Photocatalyst \rightarrow h^+ + e^-$$

whereas holes react with the hydroxyl ions to form hydroxyl radicals.

$$OH^- + h^+ \rightarrow \cdot OH$$

Superoxide anion radicals are produced by the reduction of O_2 molecules adsorbed on the catalyst surface by the photogenerated electrons.

$$O_2 + e^- \rightarrow \cdot O_2^-$$

These generated radicals participated in the photocatalytic reduction and oxidation reactions to degrade dyes.

Scavenger results showed that mainly holes are responsible for the degradation of dyes. Therefore, the dyes adsorbed at the surface of catalyst degradation achieved by direct hole oxidation by catalyst suspension (Ge et al., 2012).

$$Pollutant + h^+ \rightarrow DegradationProducts$$

Stability of the photocatalyst

The stability of the catalyst is also important for its practical applications. In order to investigate the stability of the photocatalyst, recycle experiments were carried out for pure Ag_3PO_4 and 5%$LaNiO_3/Ag_3PO_4$. After each cycle the catalyst is washed with water/ethanol to remove any adsorbed dyes on the surface. Figure 11 shows that pure Ag_3PO_4 is not stable and shows catalyst degradation even up to 2nd cycle, whereas 5% $LaNiO_3/Ag_3PO_4$ is highly stable up to five cycles with degradation efficiency greater than 85%. XRD spectra of 5% $LaNiO_3/Ag_3PO_4$ composite after five cycles were also recorded to check the stability of photocatalysts. Figure 12 shows that pure Ag_3PO_4 is decomposed to metallic Ag. While no signal from metallic Ag was observed with the 5% $LaNiO_3/Ag_3PO_4$ composite, which confirming a higher stability of 5% $LaNiO_3$/ Ag_3PO_4 composite as compared to pure Ag_3PO_4.

TABLE 2 Comparison of MO photodegradation by various catalysts from the literature.

Catalyst	Catalyst amount (mg)	Dye amount (mg/L)	Degradation time (min)	Degradation efficiency (%)	Rate constant (min^{-1})	References
$AgBr/Ag_3PO_4$	100	10	40	95.1	-	Cao et al. (2012)
Ag_3PO_4/TiO_2	40	10	60	95.5	0.052	Liu et al. (2019)
Ag_3PO_4/ g-C_3N_4	100	20	30	94	-	Hu et al. (2020)
Ag_3PO_4	50	5	30	58	-	Ge, (2014)
$LaNiO_3$	400	10	300	74.9	0.1520	Li et al. (2010)
$Ag_3PO_4/BiPO_4$	100	10	60	98	0.106	Lin et al. (2013)
Ag_3PO_4/GO	80	20	50	86.4	0.0394	Chen et al. (2013a)
Ag_3PO_4/ Nb_2O_5	500	10	60	96	0.073	Osman et al. (2021)
Ag_3PO_4/AgI	100	20	18	96.9	-	Chen et al. (2013b)
Ag/Ag_3PO_4	300	20	12	99	0.215	Liu et al. (2012)
Ag_3PO_4/rGO	20	10	210	92	0.010	Dong et al. (2013)
Ag_3PO_4/BiOI	50	10	50	98	0.109	Wang et al. (2015)
Ag_2S/Ag_3PO_4	35	10	120	99	0.0338	Tian et al. (2017)
Ag_3PO_4/ $PbBiO_2Br$	100	20	50	98	–	Xia et al. (2019)
Ag_3PO_4/ $NiFe_2O_4$	20	10	30	96.8	0.12	Huang et al. (2018)
Ag_3PO_4/MoS_2	30	20	120	98.2	0.0654	Zhu et al. (2016)
$LaNiO_3$/ Ag_3PO_4	25	50	20	99.4	0.1804	Present Study

Comparison of dyes degradation from previously reported studies

Photodegradation is proved to be a very efficient method for the removal of RhB from water. In the past, a lot of work has been done in this regard. Different Ag_3PO_4 based composites, including Ag_3PO_4@GO, Ag_3PO_4/WO_3, Ag_3PO_4/Ag, Ag_3PO_4/ZnO, Ag_3PO_4/N-TiO_2, $Ag_3PO_4/BiVO_4$, $AgBr/Ag_3PO_4$, Ag_2MoO_4/Ag_3PO_4, have been prepared and applied for visible light photocatalytic degradation of rhodamine B. These composites showed lower photocatalytic efficiency than recent study. Perovskite $LaNiO_3/Ag_3PO_4$ photocatalyst showed the highest catalytic activity for the degradation of 50 ppm RhB solution in just 20 min, with rate constant of 0.213 min^{-1} using small amount of catalyst 25 mg as shown in Table 1.

Similarly various photocatalysts have been used for MO photodegradation in the literature. Different Ag_3PO_4 based composites including $AgBr/Ag_3PO_4$, Ag_3PO_4/TiO_2, Ag_3PO_4/g-C_3N_4, $Ag_3PO_4/BiPO_4$, Ag_3PO_4/GO, Ag_3PO_4/Nb_2O_5, Ag_3PO_4/AgI, Ag/Ag_3PO_4, Ag_3PO_4/BiOI, Ag_3PO_4/MoS_2 have been synthesized and used for visible light photocatalytic degradation of MO. The present studies shows the superior catalytic efficiency in terms of catalyst amount i.e., 25 mg, MO degradation concentrations (50 mg/L), irradiation time (20 min) degradation efficiency of 99.5%, with rate constant of 0.1804 min^{-1} as shown in Table 2.

Conclusion

Highly efficient perovskite $LaNiO_3/Ag_3PO_4$ photocatalyst was successfully prepared by the facile hydrothermal method. Firstly, $LaNiO_3$ was prepared and then composite formed with Ag_3PO_4 by hydrothermal synthesis. All the synthesized photocatalysts have shown excellent results for the degradation of rhodamine B and methyl orange in a short interval of time, and almost complete degradation efficiency was achieved. Among all synthesized photocatalysts, 5% $LaNiO_3/Ag_3PO_4$ composite has been proved to be an excellent photocatalyst for the photodegradation of RhB and MO.

The average crystallite size of silver phosphate was successfully reduced from 86.52 nm to 58.19 nm by incorporating pure phase lanthanum nickelate into silver phosphate. The photooxidation activity and stability of

Ag_3PO_4 were also enhanced by the introduction of $LaNiO_3$ in Ag_3PO_4 heterojunction. Complete photodegradation of 50 mg/L solutions of both dyes using 25 mg of 5% $LaNiO_3/Ag_3PO_4$ photocatalyst were observed in just 20 min. Photodegradation of both dyes RhB and MO follows pseudo-first-order kinetics with rate constants of 0.213 and 0.1804 min^{-1}, respectively. It was observed that photocatalytic activity was completely inhibited by using a hole scavenger, which means that holes are mainly responsible for the degradation of both dyes. Photocatalyst showed the highest stability up to five cycles with degradation efficiency greater than 85%.

Data availability statement

The original contributions presented in the study are included in the article/Supplementary Material, further inquiries can be directed to the corresponding authors.

Author contributions

The role of all authors in present study is as follows: AW designed, conceived, and supervised the complete study. AA: analyzed the data and helped in compiling the results. SA, performed the experimental part and statistical analysis, and wrote the first draft. MM: wrote sections of the manuscript, MA: made a substantial contribution to the interpretation. All authors read and approved the final manuscript.

Acknowledgments

The researchers would like to thank the Deanship of Scientific Research, Qassim University for funding the publication of this project.

Conflict of interest

The authors declare that the research was conducted in the absence of any commercial or financial relationships that could be construed as a potential conflict of interest.

Publisher's note

All claims expressed in this article are solely those of the authors and do not necessarily represent those of their affiliated organizations, or those of the publisher, the editors and the reviewers. Any product that may be evaluated in this article, or claim that may be made by its manufacturer, is not guaranteed or endorsed by the publisher.

References

Akpan, U. G., and Hameed, B. H. (2009). Parameters affecting the photocatalytic degradation of dyes using TiO2-based photocatalysts: A review. *J. Hazard. Mat.* 170, 520–529. doi:10.1016/j.jhazmat.2009.05.039

Areeb, A., Yousaf, T., Murtaza, M., Zahra, M., Zafar, M. I., and Waseem, A. (2021). Green photocatalyst Cu/NiO doped zirconia for the removal of environmental pollutants. *Mat. Today Commun.* 28, 102678. doi:10.1016/j.mtcomm.2021.102678

Aziztyana, A. P., Wardhani, S., Prananto, Y. P., and Purwonugroho, D. "Optimisation of methyl orange photodegradation using TiO2-zeolite photocatalyst and H2O2 in acid condition," in Proceedings of the IOP Conference Series: Materials Science and Engineering. IOP Publishing, Kazimierz Dolny, Poland, December 2019, 042047.

Basahel, S. N., Ali, T. T., Mokhtar, M., and Narasimharao, K. (2015). Influence of crystal structure of nanosized ZrO2 on photocatalytic degradation of methyl orange. *Nanoscale Res. Lett.* 10, 73. doi:10.1186/s11671-015-0780-z

Cao, J., Luo, B., Lin, H., Xu, B., and Chen, S. (2012). Visible light photocatalytic activity enhancement and mechanism of AgBr/Ag3PO4 hybrids for degradation of methyl orange. *J. Hazard. Mat.* 217, 107–115. doi:10.1016/j.jhazmat.2012.03.002

Cao, W., An, Y., Chen, L., Qi, Z., and Compounds (2017). Visible-light-driven Ag2MoO4/Ag3PO4 composites with enhanced photocatalytic activity. *J. Alloys Compd.* 701, 350–357. doi:10.1016/j.jallcom.2016.12.436

Chen, C., Bao, R., Yang, L., Tai, S., Zhao, Y., Wang, W., et al. (2022). Application of inorganic perovskite LaNiO3 partial substituted by Ce and Cu in absorbance and photocatalytic degradation of antibiotics. *Appl. Surf. Sci.* 579, 152026. doi:10.1016/j.apsusc.2021.152026

Chen, G., Sun, M., Wei, Q., Zhang, Y., Zhu, B., and Du, B. (2013a). Ag3PO4/graphene-oxide composite with remarkably enhanced visible-light-driven photocatalytic activity toward dyes in water. *J. Hazard. Mat.* 244, 86–93. doi:10.1016/j.jhazmat.2012.11.032

Chen, Z., Wang, W., Zhang, Z., and Fang, X. (2013b). High-efficiency visible-light-driven Ag3PO4/AgI photocatalysts: Z-Scheme photocatalytic mechanism for their enhanced photocatalytic activity. *J. Phys. Chem. C* 117, 19346–19352. doi:10.1021/jp406508y

Chowdhary, P., Bharagava, R. N., Mishra, S., and Khan, N. (2020). "Role of industries in water scarcity and its adverse effects on environment and human health," in *Environmental Concerns and Sustainable Development* (Heidelberg, Germany: Springer), 235–256.

Dong, C., Wu, K.-L., Li, M.-R., Liu, L., and Wei, X.-W. (2014). Synthesis of Ag3PO4–ZnO nanorod composites with high visible-light photocatalytic activity. *Catal. Commun.* 46, 32–35. doi:10.1016/j.catcom.2013.11.018

Dong, P., Wang, Y., Cao, B., Xin, S., Guo, L., Zhang, J., et al. (2013). Ag3PO4/reduced graphite oxide sheets nanocomposites with highly enhanced visible light photocatalytic activity and stability. *Appl. Catal. B Environ.* 132, 45–53. doi:10.1016/j.apcatb.2012.11.022

Gao, J., Huang, Q., Wu, Y., Lan, Y.-Q., and Chen, B. (2021). Metal–organic frameworks for photo/electrocatalysis. *Adv. Energy Sustain. Res.* 2, 2100033. doi:10.1002/aesr.202100033

Gao, P., Tian, X., Nie, Y., Yang, C., Zhou, Z., and Wang, Y. (2019). Promoted peroxymonosulfate activation into singlet oxygen over perovskite for ofloxacin degradation by controlling the oxygen defect concentration. *Chem. Eng. J.* 359, 828–839. doi:10.1016/j.cej.2018.11.184

Ge, M. (2014). Photodegradation of rhodamine B and methyl orange by Ag3PO4 catalyst under visible light irradiation. *Chin. J. Catal.* 35, 1410–1417. doi:10.1016/s1872-2067(14)60079-6

Ge, M., Zhu, N., Zhao, Y., Li, J., and Liu, L. (2012). Sunlight-Assisted degradation of dye pollutants in Ag3PO4 suspension. *Ind. Eng. Chem. Res.* 51, 5167–5173. doi:10.1021/ie202864n

Ghafoor, A., Bibi, I., Ata, S., Majid, F., Kamal, S., Iqbal, M., et al. (2021). Energy band gap tuning of LaNiO3 by Gd, Fe and Co ions doping to enhance solar light absorption for efficient photocatalytic degradation of RhB dye: A mechanistic approach. *J. Mol. Liq.* 343, 117581. doi:10.1016/j.molliq.2021.117581

Grabowska, E. (2016). Selected perovskite oxides: Characterization, preparation and photocatalytic properties—a review. *Appl. Catal. B Environ.* 186, 97–126. doi:10.1016/j.apcatb.2015.12.035

Guan, X., and Guo, L. (2014). Cocatalytic effect of SrTiO3 on Ag3PO4 toward enhanced photocatalytic water oxidation. *ACS Catal.* 4, 3020–3026. doi:10.1021/cs5005079

Hameeda, B., Mushtaq, A., Saeed, M., Munir, A., Jabeen, U., and Waseem, A. (2021). Development of Cu-doped NiO nanoscale material as efficient photocatalyst for visible light dye degradation. *Toxin Rev.* 40, 1396–1406. doi:10.1080/15569543.2020.1725578

He, P., Song, L., Zhang, S., Wu, X., and Wei, Q. (2014). Synthesis of g-C3N4/Ag3PO4 heterojunction with enhanced photocatalytic performance. *Mat. Res. Bull.* 51, 432–437. doi:10.1016/j.materresbull.2013.12.064

Hu, Z., Lyu, J., and Ge, M. (2020). Role of reactive oxygen species in the photocatalytic degradation of methyl orange and tetracycline by Ag3PO4 polyhedron modified with g-C3N4. *Mat. Sci. Semicond. process.* 105, 104731. doi:10.1016/j.mssp.2019.104731

Huang, K., Lv, Y., Zhang, W., Sun, S., Yang, B., Chi, F., et al. (2015). One-step synthesis of Ag 3 PO 4/Ag photocatalyst with visible-light photocatalytic activity. *Mat. Res.* 18, 939–945. doi:10.1590/1516-1439.346614

Huang, S., Xu, Y., Zhou, T., Xie, M., Ma, Y., Liu, Q., et al. (2018). Constructing magnetic catalysts with *in-situ* solid-liquid interfacial photo-Fenton-like reaction over Ag3PO4@ NiFe2O4 composites. *Appl. Catal. B Environ.* 225, 40–50. doi:10.1016/j.apcatb.2017.11.045

Katheresan, V., Kansedo, J., and Lau, S. Y. (2018). Efficiency of various recent wastewater dye removal methods: A review. *J. Environ. Chem. Eng.* 6, 4676–4697. doi:10.1016/j.jece.2018.06.060

Khalid, N. R., Mazia, U., Tahir, M. B., Niaz, N. A., and Javid, M. A. (2020). Photocatalytic degradation of RhB from an aqueous solution using Ag3PO4/N-TiO2 heterostructure. *J. Mol. Liq.* 313, 113522. doi:10.1016/j.molliq.2020.113522

Lellis, B., Fávaro-Polonio, C. Z., Pamphile, J. A., and Polonio, J. C. (2019). Effects of textile dyes on health and the environment and bioremediation potential of living organisms. *Biotechnol. Res. Innovation* 3, 275–290. doi:10.1016/j.biori.2019.09.001

Li, X., Xu, P., Chen, M., Zeng, G., Wang, D., Chen, F., et al. (2019). Application of silver phosphate-based photocatalysts: Barriers and solutions. *Chem. Eng. J.* 366, 339–357. doi:10.1016/j.cej.2019.02.083

Li, Y., Yao, S., Wen, W., Xue, L., Yan, Y., and Compounds (2010). Sol–gel combustion synthesis and visible-light-driven photocatalytic property of perovskite LaNiO3. *J. Alloys Compd.* 491, 560–564. doi:10.1016/j.jallcom.2009.10.269

Lin, H., Ye, H., Xu, B., Cao, J., and Chen, S. (2013). Ag3PO4 quantum dot sensitized BiPO4: A novel p–n junction Ag3PO4/biPO4 with enhanced visible-light photocatalytic activity. *Catal. Commun.* 37, 55–59. doi:10.1016/j.catcom.2013.03.026

Liu, H., Li, D., Yang, X., and Li, H. (2019). Fabrication and characterization of Ag3PO4/TiO2 heterostructure with improved visible-light photocatalytic activity for the degradation of methyl orange and sterilization of *E. coli*. *Mater. Technol.* 34, 192–203. doi:10.1080/10667857.2018.1545391

Liu, R., Li, H., Duan, L., Shen, H., Zhang, Q., and Zhao, X. (2018). The synergistic effect of graphene oxide and silver vacancy in Ag3PO4-based photocatalysts for rhodamine B degradation under visible light. *Appl. Surf. Sci.* 462, 263–269. doi:10.1016/j.apsusc.2018.07.173

Liu, Y., Fang, L., Lu, H., Li, Y., Hu, C., and Yu, H. (2012). One-pot pyridine-assisted synthesis of visible-light-driven photocatalyst Ag/Ag3PO4. *Appl. Catal. B Environ.* 115, 245–252. doi:10.1016/j.apcatb.2011.12.038

Luo, J., Zhang, S., Sun, M., Yang, L., Luo, S., and Crittenden, J. C. (2019). A critical review on energy conversion and environmental remediation of photocatalysts with remodeling crystal lattice, surface, and interface. *ACS Nano* 13, 9811–9840. doi:10.1021/acsnano.9b03649

Lv, T., Wu, M., Guo, M., Liu, Q., and Jia, L. (2019). Self-assembly photocatalytic reduction synthesis of graphene-encapusulated LaNiO3 nanoreactor with high efficiency and stability for photocatalytic water splitting to hydrogen. *Chem. Eng. J.* 356, 580–591. doi:10.1016/j.cej.2018.09.031

Maheshwari, K., Agrawal, M., and Gupta, A. B. (2021). "Dye pollution in water and wastewater," in *Novel materials for dye-containing wastewater treatment*. Editors S. S. Muthu and A. Khadir (Heidelberg, Germany: Springer), 1–25.

Mansouri, M., Mozafari, N., Bayati, B., and Setareshenas, N. (2019). Photocatalytic dye degradation of methyl orange using zirconia–zeolite nanoparticles. *Bull. Mat. Sci.* 42, 230–311. doi:10.1007/s12034-019-1933-y

Markandeya, S., Shukla, S., and Mohan, D. (2017). Toxicity of disperse dyes and its removal from wastewater using various adsorbents: A review. *Res. J. Environ. Toxicol.* 11, 72–89. doi:10.3923/rjet.2017.72.89

Masnadi-Shirazi, M., Lewis, R., Bahrami-Yekta, V., Tiedje, T., Chicoine, M., and Servati, P. (2014). Bandgap and optical absorption edge of GaAs1− xBix alloys with 0< x< 17.8. *J. Appl. Phys.* 116, 223506.

Osman, N. S., Sulaiman, S. N., Muhamad, E. N., Mukhair, H., Tan, S. T., and Abdullah, A. H. (2021). Synthesis of an Ag3PO4/Nb2O5 photocatalyst for the degradation of dye. *Catalysts* 11, 458. doi:10.3390/catal11040458

Qi, X., Gu, M., Zhu, X., Wu, J., Wu, Q., Long, H., et al. (2016). Controlled synthesis of Ag3PO4/BiVO4 composites with enhanced visible-light photocatalytic performance for the degradation of RhB and 2, 4-DCP. *Mat. Res. Bull.* 80, 215–222. doi:10.1016/j.materresbull.2016.03.025

Reunchan, P., and Umezawa, N. (2013). Native defects and hydrogen impurities in Ag3PO4. *Phys. Rev. B* 87, 245205. doi:10.1103/physrevb.87.245205

Saravanan, A., Kumar, P. S., Vo, D.-V. N., Yaashikaa, P. R., Karishma, S., Jeevanantham, S., et al. (2020). Photocatalysis for removal of environmental pollutants and fuel production: A review. *Environ. Chem. Lett.* 19, 441–463. doi:10.1007/s10311-020-01077-8

Sudha, D., and Sivakumar, P. (2015). Review on the photocatalytic activity of various composite catalysts. *Chem. Eng. Process. Process Intensif.* 97, 112–133. doi:10.1016/j.cep.2015.08.006

Szczepanik, B. (2017). Photocatalytic degradation of organic contaminants over clay-TiO2 nanocomposites: A review. *Appl. Clay Sci.* 141, 227–239. doi:10.1016/j.clay.2017.02.029

Tian, J., Yan, T., Qiao, Z., Wang, L., Li, W., You, J., et al. (2017). Anion-exchange synthesis of Ag2S/Ag3PO4 core/shell composites with enhanced visible and NIR light photocatalytic performance and the photocatalytic mechanisms. *Appl. Catal. B Environ.* 209, 566–578. doi:10.1016/j.apcatb.2017.03.022

Wang, B., Gu, X., Zhao, Y., and Qiang, Y. (2013). A comparable study on the photocatalytic activities of Ag3PO4, AgBr and AgBr/Ag3PO4 hybrid microstructures. *Appl. Surf. Sci.* 283, 396–401. doi:10.1016/j.apsusc.2013.06.121

Wang, Y., Cheng, X., Meng, X., Feng, H., Yang, S., Sun, C., et al. (2015). Preparation and characterization of Ag3PO4/BiOI heterostructure photocatalyst with highly visible-light-induced photocatalytic properties. *J. Alloys Compd.* 632, 445–449. doi:10.1016/j.jallcom.2014.11.231

Waseem, A., Arshad, J., Iqbal, F., Sajjad, A., Mehmood, Z., and Murtaza, G. (2014). Pollution status of Pakistan: A retrospective review on heavy metal contamination of water, soil, and vegetables. *Biomed. Res. Int.* 2014, 813206. doi:10.1155/2014/813206

Wu, Y., Li, Y., Gao, J., and Zhang, Q. (2021). Recent advances in vacancy engineering of metal-organic frameworks and their derivatives for electrocatalysis. *SusMat* 1, 66–87. doi:10.1002/sus2.3

Xia, Y., He, Z., and Su, J. (2019). One-step construction of novel Ag3PO4/PbBiO2Br composite with enhanced photocatalytic activity. *Mat. Res. Express* 6, 085909. doi:10.1088/2053-1591/ab1f44

Xu, H., Wang, C., Song, Y., Zhu, J., Xu, Y., Yan, J., et al. (2014). CNT/Ag3PO4 composites with highly enhanced visible light photocatalytic activity and stability. *Chem. Eng. J.* 241, 35–42. doi:10.1016/j.cej.2013.11.065

Zhang, C., Wang, L., Yuan, F., Meng, R., Chen, J., Hou, W., et al. (2020). Construction of pn type Ag3PO4/CdWO4 heterojunction photocatalyst for visible-light-induced dye degradation. *Appl. Surf. Sci.* 534, 147544. doi:10.1016/j.apsusc.2020.147544

Zhang, G., Liu, G., Wang, L., and Irvine, J. T. (2016). Inorganic perovskite photocatalysts for solar energy utilization. *Chem. Soc. Rev.* 45, 5951–5984. doi:10.1039/c5cs00769k

Zhang, J., Yu, K., Yu, Y., Lou, L.-L., Yang, Z., Yang, J., et al. (2014). Highly effective and stable Ag3PO4/WO3 photocatalysts for visible light degradation of organic dyes. *J. Mol. Catal. A Chem.* 391, 12–18. doi:10.1016/j.molcata.2014.04.010

Zhang, Z., Shao, S., Dang, J., Lu, C., Qin, F., and Guan, W. (2017). Synthesis of ZnWO4/Ag3PO4 p–n heterojunction photocatalyst and enhanced visible-light photocatalytic applications. *Water Sci. Technol.* 77, 1204–1212. doi:10.2166/wst.2017.631

Zheng, C., Yang, H., Cui, Z., Zhang, H., and Wang, X. (2017). A novel Bi4Ti3O12/Ag3PO4 heterojunction photocatalyst with enhanced photocatalytic performance. *Nanoscale Res. Lett.* 12, 608–612. doi:10.1186/s11671-017-2377-1

Zhu, C., Zhang, L., Jiang, B., Zheng, J., Hu, P., Li, S., et al. (2016). Fabrication of Z-scheme Ag3PO4/MoS2 composites with enhanced photocatalytic activity and stability for organic pollutant degradation. *Appl. Surf. Sci.* 377, 99–108. doi:10.1016/j.apsusc.2016.03.143